ATLAS NOTE

ATLAS-CONF-2011-076

May 28, 2011

A Search for Lepton-Jets with Muons in pp Collisions at $\sqrt{s} = 7$ TeV in the ATLAS Detector

The ATLAS collaboration

Abstract

We present a search for a new, light ($\sim$1 GeV) hidden-valley boson decaying to muons in a final state consisting of collimated leptons (lepton-jets). The analysis is performed on 40 pb^{-1} of proton-proton collisions recorded by the ATLAS detector at the LHC with $\sqrt{s} = 7$ TeV. Events are required to contain at least two isolated lepton-jets, each of which must contain at least two muons. We observe no candidate events after event selection, while expecting 0.20 ± 0.19 background events. We set 95% C.L. upper limits on the cross-section for supersymmetric events with the lightest supersymmetric particle decaying to the new boson, of between 1.1 and 3.1 pb, as a function of the new boson mass.

1 Introduction

Several recent observations of abundances of cosmic electrons and positrons [1–3] have reported unexpected large rates. Signals from some direct dark matter detection experiments [4, 5] also show unexplained excesses over backgrounds. A new, light (GeV-scale), boson in a hidden sector weakly-coupled to the Standard Model (SM) has been proposed to explain these anomalies [6]. At high-energy colliders, the phenomenology of such models has been studied extensively [7–11]. In general the proposed new boson (the dark photon, γ_d) has a mass less than $\sim$2 GeV (to prevent decays to protons), decays into SM fermion pairs, and in many models decays promptly.

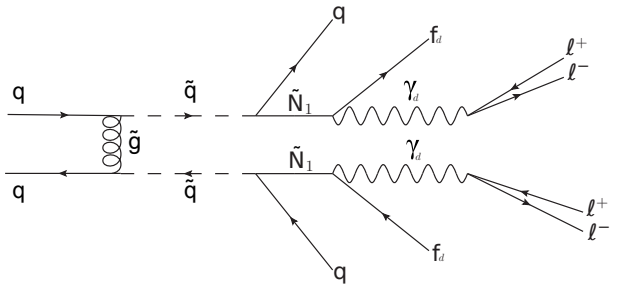

Figure 1: A Feynman diagram demonstrating one of the production mechanisms of lepton-jets from squark pairs. The lightest supersymmetric particle (shown here as $\tilde{N}_1$) decays to a dark photon (γ_d) that produces a pair of leptons, and a dark fermion (f_d) (carrying SUSY R-parity) that escapes undetected but may radiate extra dark photons.

These new proposals have a dramatic impact on SUSY signatures at high-energy colliders since the Lightest Supersymmetric Particle (LSP) is no longer stable with R-parity conservation. Instead, it is allowed to decay into the dark sector, producing a dark photon and a dark fermion (carrying SUSY R-parity), both of which have GeV-scale mass (see Figure 1). As the hidden sector particles are light compared to the squark masses, they are boosted and their decays result in jets of tightly collimated particles from the γ_d. In the case where the dark boson mass $m_a < 2 \cdot m(\pi^{\pm})$ such jets consist exclusively of leptons. Even for higher γ_d masses, the lepton content of the jets is high, so we will also refer to them as lepton-jets. Every SUSY event in this scenario will have at least two tightly collimated lepton-jets, as well as significant missing transverse energy ($E_{\mathrm{T}}^{\mathrm{miss}}$) from the dark fermion. Searches for this final state were performed by DØ [12], and more recently by CMS [13]. Dark photons could be produced by a number of processes, such as electrowino pair-production or rare non-SM Z decays. We investigate here the pair-production of squarks/gluinos, which each cascade-decay to a LSP plus a jet, because the cross-section is large with respect to other possible processes if the squarks/gluinos are light enough. But we do not apply any requirements on the $E_{\mathrm{T}}^{\mathrm{miss}}$ in this analysis, since other lepton-jet production processes could have little $E_{\mathrm{T}}^{\mathrm{miss}}$.

Radiation of dark photons from the dark fermion may produce more soft leptons [7], thus increasing the lepton multiplicities. (In closely related models, dark radiation could also come from a dark Higgs boson, or even the dark photon itself.) The amount of radiation is determined by the parameter α_d, the coupling within the dark sector. Small values of α_d will produce a fairly simple lepton-jet with two leptons. Larger values of α_d may produce lepton-jets with additional prompt muon pairs, draining the boost. We consider benchmark values of $\alpha_d = 0.0$, 0.1, and 0.3 and boson masses of $m_a = 300$ and 500 MeV.

Data were collected during the 2010 run of proton-proton collisions at the LHC with $\sqrt{s} = 7$ TeV by the ATLAS detector [14] and correspond to 40 pb^{-1} of integrated luminosity [15]. We examine events that have two well-isolated lepton-jets, each containing at least two muons. The isolation is calculated

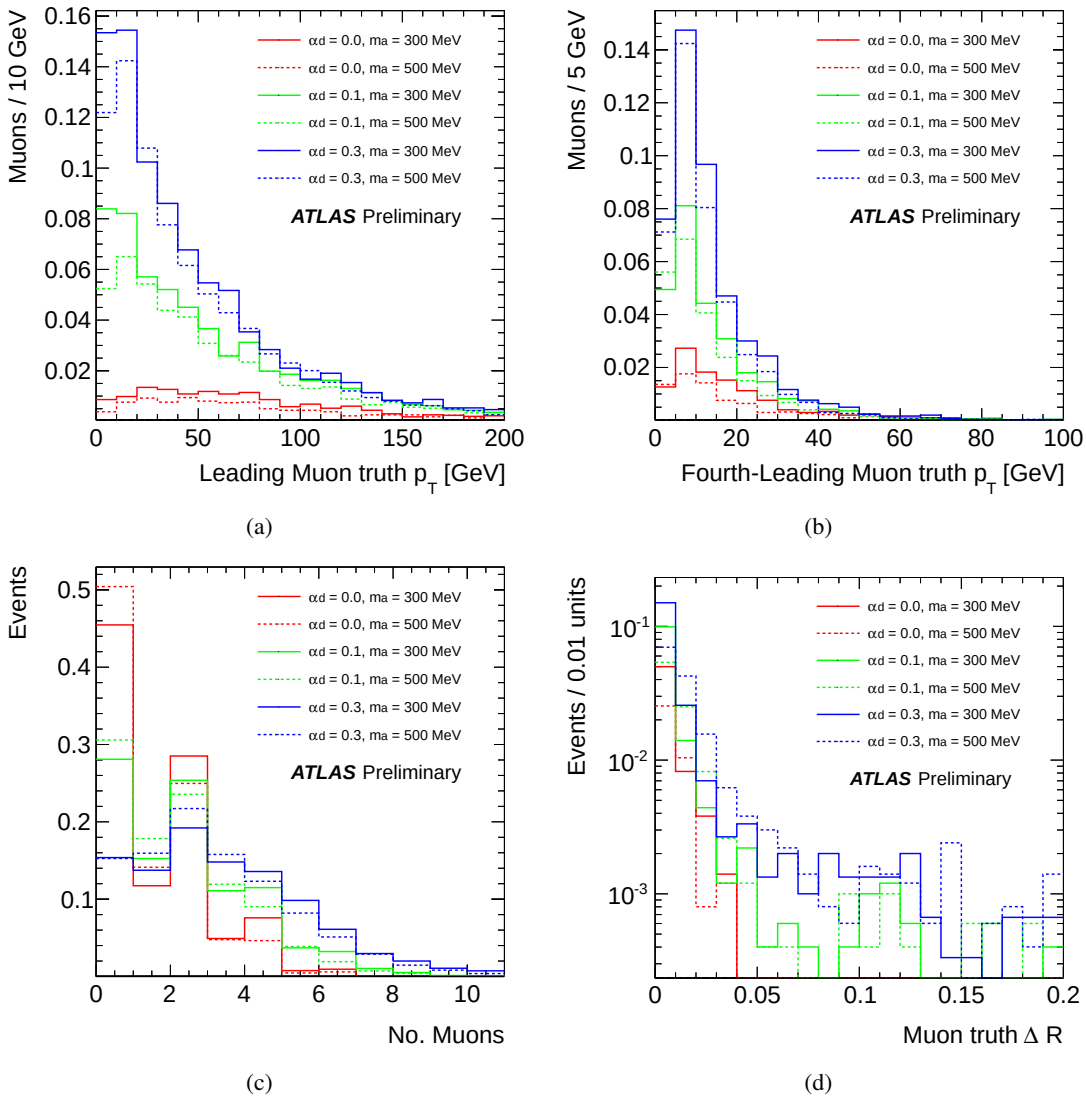

Figure 2: (a) The generator-level Monte Carlo p_{T} spectrum of the leading muon produced by the dark photon decay; (b) the generator-level Monte Carlo p_{T} spectrum of the fourth muon after requiring three such muons with $p_{\mathrm{T}} > 7$ GeV; (c) the number of generator-level Monte Carlo muons above 7 GeV per event; and (d) the separation between the two closest such muons. The samples are normalized to an arbitrary luminosity.

taking into account the proximity of the muons to each other. The analysis is designed to extract the signal from SM backgrounds, the largest of which is QCD multi-jet production.

2 Monte Carlo Simulation

2.1 Signal Samples

The signal Monte Carlo (MC) events were generated by Itay Yavin and provided as Les Houches Event (LHE) files [16, 17]. The SUSY production process and cascade decay to the dark sector are modeled using MADGRAPH [18]. A custom Mathematica package handles the dark-sector showering. The result-

ing LHE files were then processed by PYTHIA version 6.4 [19]. The SPS1a benchmark was used for the SUSY parameters [20] (details in Table 1). The specifics of the SPS1a parameters have little impact on the generality of the signal sample, though the squark mass does determine the signal cross-section.

The generator-level p_{T} distributions of muons in the MC signal samples are shown in Figure 2. Also shown are the number of these generator-level muons per event which have $p_{\mathrm{T}} > 7$ GeV, and the ΔR $(= \sqrt{(\Delta\phi)^2 + (\Delta\eta)^2})$ separation between the two closest such muons.

	χ^0	$\tilde{g}$	$\tilde{q}$
Mass	96.1 GeV	595 GeV	520 GeV

Table 1: The masses of the χ^0, $\tilde{g}$, and $\tilde{q}$ in the SPS1a benchmark. Here χ_0 corresponds to $\tilde{N}_1$ in Figure 1.

2.2 Background Samples and Normalization

The MC event samples for SM backgrounds were generated using a mix of PYTHIA (QCD di-jets, W+Jets, and Z+Jets) and MC@NLO [21] ($t\bar{t}$, WW, WZ, and ZZ). Each of the background and signal MC simulation samples was processed through the ATLAS detector-response simulation based on GEANT4 [22] [23]. The events were then reconstructed using the same analysis chain as the data. The various samples are listed in Table 2. Since PYTHIA calculates cross-sections to leading order (LO), a k-factor is used to scale the rates of the W+Jets and Z+Jets samples to next-to-next-to-leading order (NNLO) [24]. The $t\bar{t}$ and di-boson samples are normalized using the NLO cross-section.

The largest background is expected to come from QCD events, due to its large cross-section. The size of the QCD background is estimated by requiring that the invariant mass of the MC simulation and data agree for events with exactly two reconstructed muons around the J/Ψ peak ($3 < M_{\ell\ell} < 4$ GeV), the Υ peak ($9 < M_{\ell\ell} < 10$ GeV), and the QCD-dominated continuum region ($20 < M_{\ell\ell} < 40$ GeV). The J/Ψ and Υ events are separated from the bulk of the QCD MC events using the generator-level MC information. The normalization is calculated for each of the reference regions by solving a system of three linear equations. The resultant scale factors are 0.11 for the J/Ψ, 0.076 for the Υ, and 0.45 for the QCD region. The invariant mass distribution for events with two muons, after the QCD normalization, is shown in Figure 3.

Two QCD MC samples are used: an inclusive sample and a sample with a generator-level filter requiring ≥ 1 muon. The inclusive sample is used for the background acceptance studies, whereas the ≥ 1 muon sample is used to model the background after all analysis requirements.

3 Event Selection

3.1 Trigger Selection

The data for this analysis were collected from July 29$^{\mathrm{th}}$ to October 29$^{\mathrm{th}}$, 2010 and represent an integrated luminosity of 40 ± 1 pb^{-1}. They were recorded during LHC stable-beam conditions when the ATLAS detector components relevant to this analysis were operating within normal conditions. Due to the large increase in instantaneous luminosity during the 2010 LHC operation, the prescales applied to the low-p_{T} threshold single and di-muon trigger requirements grew very quickly. We select events passing a trigger that requires two separated muons with $p_{\mathrm{T}} \geq 6$ GeV and $|\eta| < 2.4$. Of the trigger requirements that were un-prescaled during the entire data-taking period, this is the one with the greatest acceptance for our signal. The trigger decision is included in the simulation and MC events are required to satisfy the same trigger conditions.

Physics process	Generator	$\sigma * \mathrm{BR}$ (pb)	NNLO k-factor	N Events
QCD	PYTHIA	Normalized in Data	–	11059397
QCD ($\rightarrow \geq 1\ \mu$)	PYTHIA	Normalized in Data	–	3006684
W+Jets ($\rightarrow \mu\nu$)	PYTHIA	8940	1.17	999334
Z+Jets ($\rightarrow \mu^+\mu^-$)	PYTHIA	856	1.13	298952
$t\bar{t}$ (inclusive)	MC@NLO	144	–	974401
WW ($\rightarrow \mu\nu\mu\nu$)	MC@NLO	0.506	–	49939
WZ ($\rightarrow \ell\nu\ell'\ell'$)	MC@NLO	0.165	–	24997
ZZ ($\rightarrow \ell\ell\ell'\ell'$)	MC@NLO	0.273	–	99986
Squark Signal Samples			–	
$\alpha_d = 0.0$, $m_a = 300$ ($\rightarrow \geq 4\mu$)	MADGRAPH & PYTHIA	0.121	–	4984
$\alpha_d = 0.0$, $m_a = 500$ ($\rightarrow \geq 4\mu$)	MADGRAPH & PYTHIA	0.0795	–	4998
$\alpha_d = 0.1$, $m_a = 300$ ($\rightarrow \geq 4\mu$)	MADGRAPH & PYTHIA	0.291	–	4994
$\alpha_d = 0.1$, $m_a = 500$ ($\rightarrow \geq 4\mu$)	MADGRAPH & PYTHIA	0.234	–	4996
$\alpha_d = 0.3$, $m_a = 300$ ($\rightarrow \geq 4\mu$)	MADGRAPH & PYTHIA	0.537	–	2998
$\alpha_d = 0.3$, $m_a = 500$ ($\rightarrow \geq 4\mu$)	MADGRAPH & PYTHIA	0.470	–	4987

Table 2: The background and signal Monte Carlo samples used in the analysis, showing the generator, cross-section times branching ratio, k-factor (where relevant) and number of simulated events. The generated final-state of the MC sample is specified in parentheses, where ℓ refers to either e or μ.

3.2 Muon Selection

We consider two sets of quality requirements for reconstructed muons. Selected muons must minimally:

- have a track reconstructed in the Muon Spectrometer (MS);
- have an Inner Detector (ID) track matched to the MS track within the tracking coverage, $|\eta| \leq 2.5$;
- have $p_{\mathrm{T}} > 7$ GeV.

To reduce the impact of muons from background sources, such as decays-in-flight of mesons, events in the final signal region are required to contain a minimum of three "high-quality" reconstructed muons, which must also satisfy:

- additional ID track requirements;
- the χ^2 per degree of freedom of the match between the MS and ID tracks must be less than 5.

These additional requirements serve to reject muon candidates that lack a sufficient number of hits in the tracking system or are not compatible with tracks produced at the primary vertex having traversed the entire ID.

Candidate events are required to contain at least four muons, of which at least three must be high-quality. These requirements are motivated by Figure 4, which shows the distributions of the number of muons and high-quality muons in the selected events. The background from cosmic muons is negligible after these requirements.

To ensure the trigger efficiencies are well-understood, we require that the selected muons in each candidate event include the two muons satisfying our trigger. The p_{T} requirement insulates us from the turn-on region of the di-muon trigger efficiency. Additionally, the QCD muon p_{T} spectrum rises steeply with decreasing muon p_{T} so that loosening the p_{T} requirement on the sub-leading muons does not improve the sensitivity of the search.

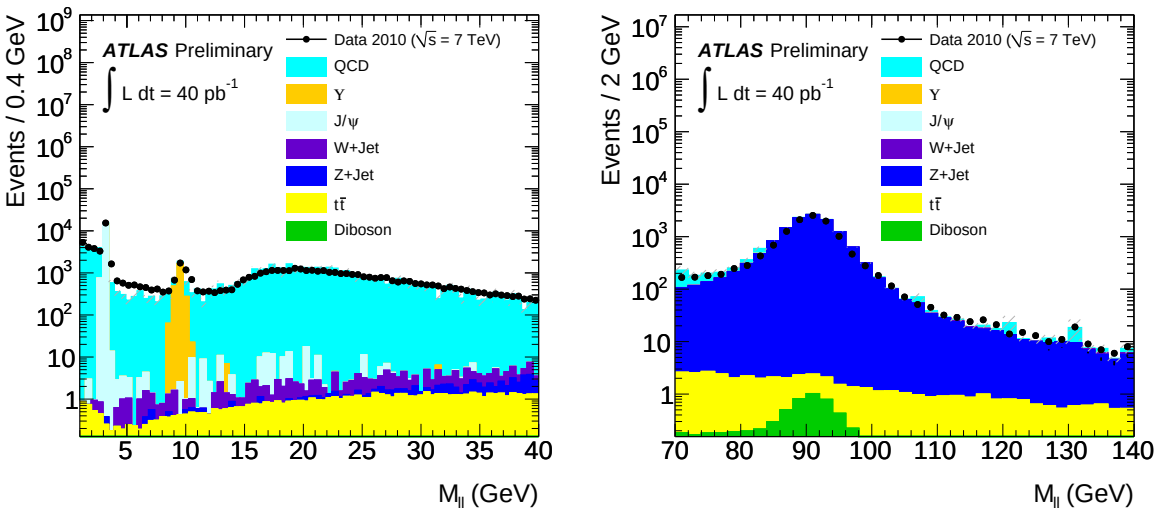

(a) (b)

Figure 3: (a) The di-lepton invariant mass distribution with the regions used to normalize the QCD MC. (b) The di-lepton invariant mass distribution around the Z peak, normalized to 40 pb^{-1}. The statistical error on the MC is represented by the grey hatched markings.

3.2.1 Muon Efficiency Measurement

The normalization of the SM MC simulation is cross-checked by comparing the numbers of data and simulated events within a window around the Z invariant mass peak (see Figure 3). The ratio of data to MC events is 1.03 (after including the the muon p_{T} smearing discussed in Section 5.2). The remaining 3% difference is consistent with the systematic uncertainties associated with the luminosity, trigger, and reconstruction systematics.

The efficiency of the high-quality muon selection is further investigated using the tag-and-probe method in events around both the J/Ψ and Z invariant mass peaks. Good agreement between the data and simulation is observed within the statistical uncertainties. This comparison between data and MC is statistically limited for muon pairs with separation $\Delta R < 0.01$. Muon pairs from the signal populate this region of small ΔR, so we must rely solely on the MC to predict any possible variation in muon reconstruction efficiency with small separation between the muons in the lepton-jet. The MC predicts a slight systematic variation of muon reconstruction efficiency with ΔR, which is not completely understood. We assign a 4% systematic uncertainty on the efficiency per lepton-jet to account for any deficiencies in the simulation of reconstruction of closely separated muons.

3.3 Lepton-Jet Clustering

The lepton-jets are reconstructed using an iterative cone algorithm as follows:

1. The reconstructed muons (passing the minimal requirements of Section 3.2) are collected in a p_{T}-ordered list of "available muons."

2. The available muon with the highest p_{T} is selected as the seed for a new lepton-jet and is removed from the list of available muons.

3. The available muons are looped over. Each subsequent muon with $\Delta R < 0.1$ from the center of the

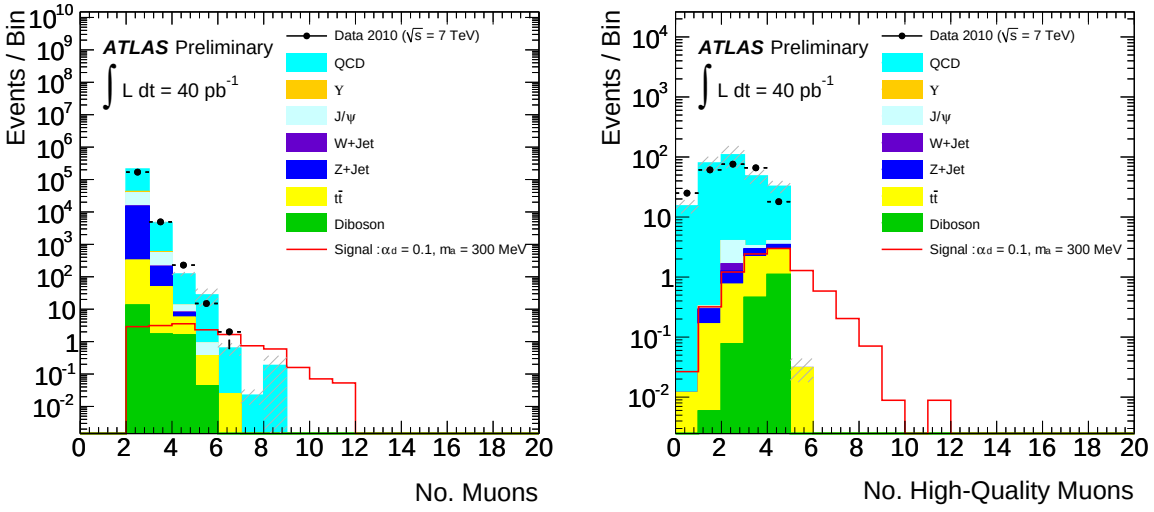

(a) (b)

Figure 4: (a) The distribution of the number of reconstructed muons after the trigger requirement and requiring ≥ 2 such muons. (b) The distribution of the number of high-quality muons after additionally requiring ≥ 4 reconstructed muons. The signal for $\alpha_d = 0.1$, $m_a = 300$ MeV has been overlaid in red. Candidate events are required to have ≥ 4 reconstructed muons and ≥ 3 high-quality muons. The statistical error on the MC is represented by the grey hatched markings.

seed is added to the lepton-jet, forming a composite object out of the vector sum of their momenta, adjusting the seed direction, and removing the added muon from the list of available muons.

4. When no more available muons are within the ΔR cone, return to step 2.

This process is continued until all muons have been assigned to a lepton-jet. For consideration in the analysis, candidate lepton-jets are required to have two or more muons, of which at least one muon must be high-quality. The distribution of the number of lepton-jets after requiring ≥ 4 muons in each event, of which ≥ 3 must satisfy the high-quality requirements, is shown in Figure 5. The lepton-jet p_{T} distribution is shown for events with ≥ 1 and ≥ 2 lepton-jets in Figure 6. For events with ≥ 2 lepton-jets, we show the distributions of the number of muons per lepton-jet in Figure 7 and the invariant mass of the two leading leptons in the lepton-jet in Figure 8.

3.4 Lepton-Jet Isolation

Candidate muons are expected to deposit their energy in the calorimeter uniformly within a small region of ΔR. On the other hand, muons produced in flight from hadronic decays or faked by instrumental effects will have more energy distributed around the path of the muon from other associated particles. Muon isolation in the calorimeter is calculated by considering all cells along the path of the muon through the calorimeter. The path is extrapolated by combining information from the MS and the ID [25]. A collection is made of all the cells with edges within a $\Delta R < 0.3$ cone of any muon in the lepton-jet. The cells that have an edge within $\Delta R < 0.05$ of the muons are dropped from the collection before computing the scalar sum of the calorimeter E_T, as illustrated in Figure 9.

Scaled isolation is defined as E_T^{cone}/p_T: the energy in the isolation region of each lepton-jet, divided by the p_{T} of the lepton-jet. $S/\sqrt{S+B}$ is used as a metric to select the requirement for the lepton-jet

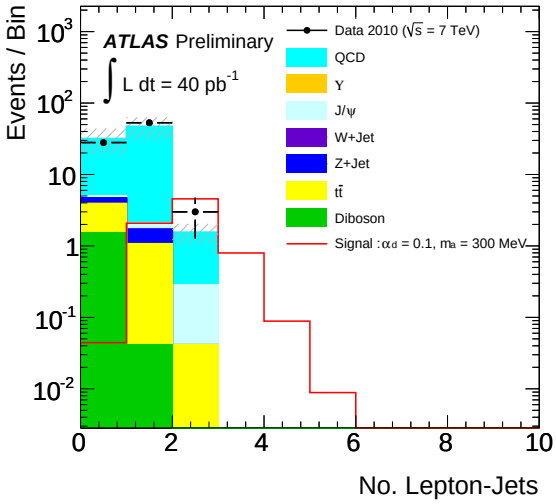

Figure 5: Distribution of the number of lepton-jets after requiring ≥ 4 muons in the event, of which ≥ 3 must satisfy the high-quality requirements. The signal MC with dark-sector showering parameter $\alpha_d = 0.1$ and dark-photon mass $m_a = 300$ MeV is shown overlaid in red. Candidate events are required to have ≥ 2 such lepton-jets. The statistical error on the MC is represented by the grey hatched markings.

isolation, resulting in a scaled isolation requirement of < 0.7. The value was optimized using a sample with looser muon quality, to get better background statistics. This predominantly removes background due to QCD, as shown in Figure 10.

4 QCD Background Estimation

The fraction of QCD di-jet events with high-p_T, isolated muons from QCD jets is expected to be very low, but the QCD cross-section is so large that this background must be carefully considered. We use here a hybrid approach, using both the data and MC simulation to estimate the size of the QCD background. Our primary method, and a cross-check to measure possible method bias, are briefly described here:

1. In our primary method, we use the data to measure the probability of reconstructing a fake muon. The fake rates are used to (a) check that the reconstructed muon multiplicity spectrum in the MC needs no further corrections and (b) calculate the probability that an MC event would satisfy our high-quality muon selection. Finally, in this method, the isolation requirement is modeled using the MC.

2. In our cross-check, we reverse the requirements on the p_{T} of the third and fourth sub-leading muons and the isolation of the two leading lepton jets. In so doing, we construct three independent, background dominated, side-band regions. By considering the fraction of events in each of the side-bands, we estimate the number of QCD events which should remain after our analysis requirements.

A more in-depth explanation of these two approaches follows.

4.1 Background Rate Measurement

The fake-muon probability is evaluated using the tag-and-probe method in a background-dominated data sample where we require two back-to-back jets with $p_{\mathrm{T}} > 25$ GeV and $|\Delta\phi| > 2$ and that there be no

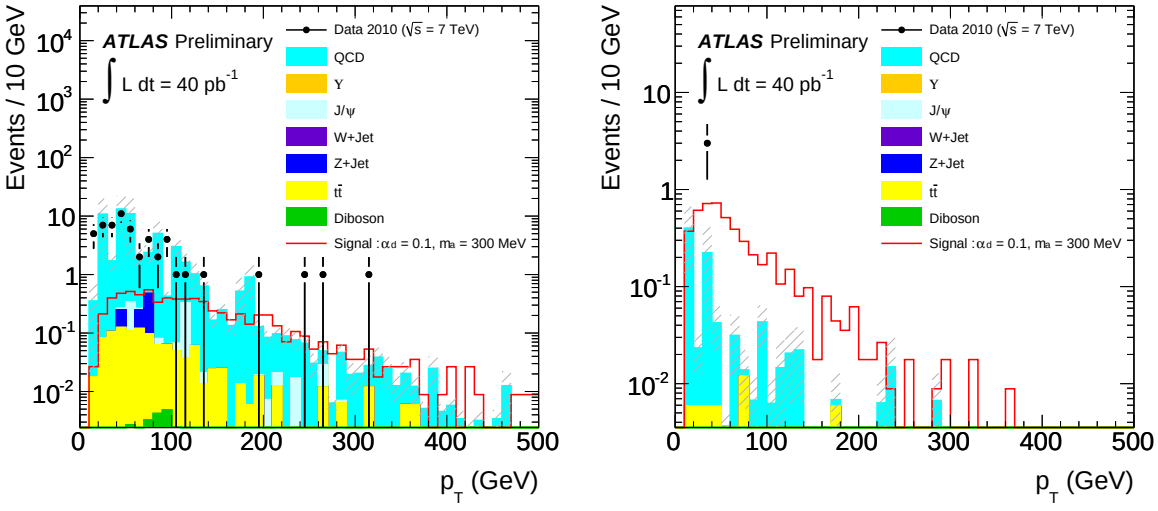

(a) (b)

Figure 6: (a) The p_{T} distribution of the leading p_{T} lepton-jet after requiring ≥ 4 muons, with ≥ 3 high-quality, in events with ≥ 1 lepton-jet. (b) The p_{T} distribution of the second-leading p_{T} lepton-jet after additionally requiring ≥ 2 lepton-jets per event. The signal MC with dark-sector showering parameter $\alpha_d = 0.1$ and dark-photon mass $m_a = 300$ MeV is shown overlaid in red. Note that due to the small fraction of events with muons, the QCD MC has large statistical uncertainties. The statistical error on the MC is represented by the grey hatched markings.

muons in the event with distance $\Delta R > 0.7$ of the probe jet. In our estimation of the QCD $\rightarrow 4$ muon background, we consider both real muons (e.g. from b decays or decays in flight) and instrumental fakes (e.g. from hadron punch-through or mis-identification).

The background data is selected using an OR of all di-jet triggers and required to contain exactly two jets with $p_{\mathrm{T}} > 25$ GeV. The requirement on the jet p_{T} removes the region dominated by the turn-on of the lowest p_{T} trigger.

In addition, we require $E_{\mathrm{T}}^{\mathrm{miss}} < 30$ GeV to remove W+Jets events that could bias our fake-muon probability measurement. We vary the value of the $E_{\mathrm{T}}^{\mathrm{miss}}$ requirement up and down by 10 GeV and find that the calculated fake-muon probability changes by about 3%.

One of the two jets is randomly selected as the tag jet and is required to contain no identified muons. The jet opposite the tag jet is then probed, looking for zero, one, or two close ($\Delta R < 0.1$) reconstructed muons. We also record how many of the muons satisfy the high-quality requirements. From this information we calculate the probability that a jet contains n fake muons ($p(n)$), and the probability that m of these are high-quality muons ($p(m|n)$).

The study is also performed on the inclusive QCD MC sample, without the generator-level muon filter. An OR of all di-jet triggers is also required in this sample, and the MC events are then re-weighted to match the jet p_{T} spectrum in the data. The fake-muon probability $p(n)$ measured in the data and MC simulation agree, within statistics, so no additional correction is applied to the muon multiplicity spectrum. The probability $p(m|n)$, is used to estimate the size of the QCD background in the final region, as described below.

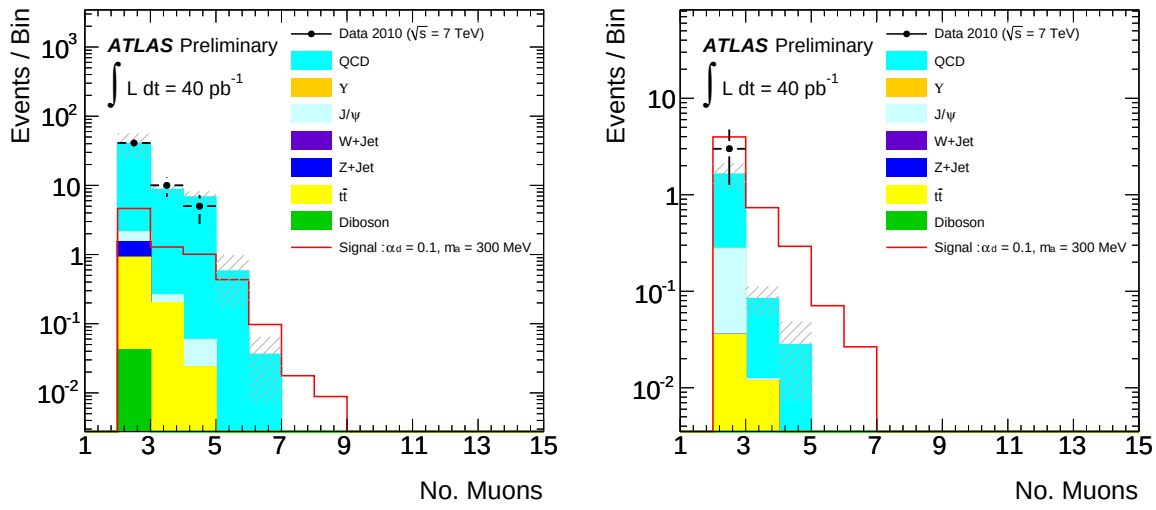

(a) (b)

Figure 7: (a) Distribution of the number of leptons in the leading p_{T} lepton-jet after requiring ≥ 4 muons, with ≥ 3 high-quality. (b) Distribution of the second-leading p_{T} lepton-jet after additionally requiring ≥ 2 lepton-jets. The signal MC with dark-sector showering parameter $\alpha_d = 0.1$ and dark-photon mass $m_a = 300$ MeV is shown overlaid in red. The statistical error on the MC is represented by the grey hatched markings.

4.2 Probabilistic Background Estimation

The QCD MC sample suffers from poor statistics after requiring ≥ 4 muons, with ≥ 3 high-quality in two lepton-jets. To recover some of the QCD sample statistics we replace the high-quality muon requirements with an event weight (w) equal to the probability the event would have passed the high-quality requirements. This weight is calculated using the measured values of $p(m|n)$. By doing this, we are able to increase the QCD MC statistics in the final region by a factor of about five.

For an event to pass the quality requirements, it must fall into one of the following three categories containing at least four muons, listed here along with their associated event weight (w):

1. Contains two lepton-jets: $w = 0.21$
2. Contains one lepton-jet and two lone muons: $w = 0.38$
3. Contains no lepton-jets and four lone muons: $w = 0.47$

This method predicts that 0.19 ± 0.19 QCD events will be found after all analysis requirements.

4.3 Control Region Based Estimation

In this section, we use the so-called ABCD method to cross-check the QCD background predictions after the final requirement on the isolation of the lepton-jets. We define four orthogonal selection regions by reversing the p_{T} and/or isolation requirements:

(A) Signal region ≥ 4 muons with ≥ 3 high-quality. Two lepton-jets with scaled isolation ≤ 0.7 and the four leading muons with $p_{\mathrm{T}} \geq 7$ GeV.

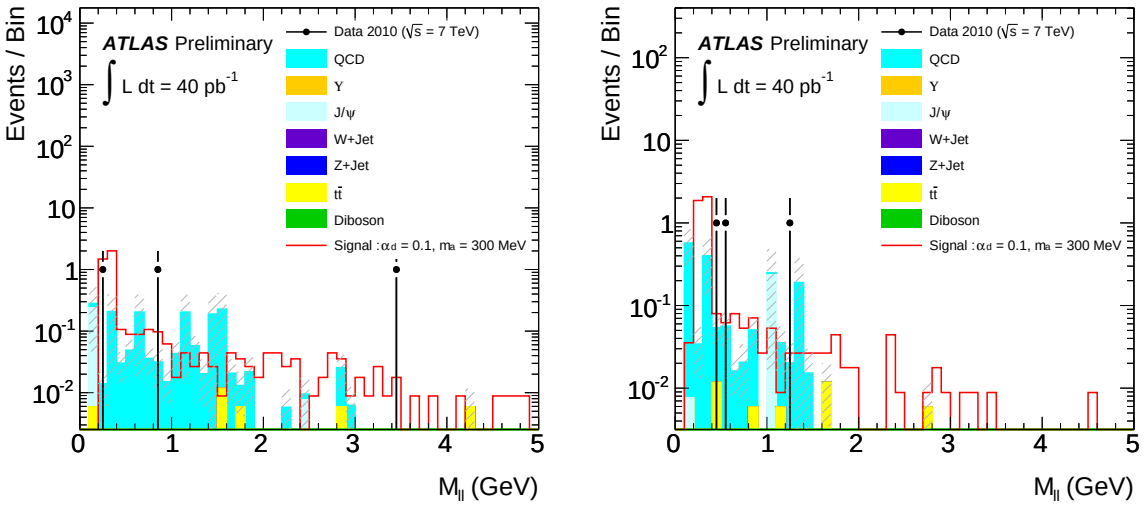

Figure 8: (a) Distribution of the di-lepton invariant mass of the leading p_{T} lepton-jet after requiring ≥ 4 muons, with ≥ 3 high-quality and ≥ 2 lepton-jets. (b) The second-leading p_{T} lepton-jet invariant mass distribution with the same requirements. The signal MC with dark-sector showering parameter $\alpha_d = 0.1$ and dark-photon mass $m_a = 300$ MeV is shown overlaid in red. Note that due to the small fraction of events with muons, the QCD MC contribution has large statistical uncertainties. The statistical error on the MC is represented by the grey hatched markings.

(B) Anti-p_{T} region ≥ 4 muons with ≥ 3 high-quality. Two lepton-jets with scaled isolation ≤ 0.7. The p_{T} requirement requirement on the third and following muons is changed to be $4 < p_{\mathrm{T}} < 7$ GeV.

(C) Anti-Isolation region ≥ 4 muons with ≥ 3 high-quality. Two lepton-jets, of which one or more must fail the scaled isolation ≤ 0.7 requirement. The p_{T} of all four muons must be ≥ 7 GeV.

(D) Anti-Both region ≥ 4 muons with ≥ 3 high-quality. Two lepton-jets, of which one or more must fail the scaled isolation ≤ 0.7 requirement. The third and following muons must lie in the $4 < p_{\mathrm{T}} < 7$ GeV window.

In the ABCD method it is very important that there is one dominan background (QCD in this case) and that the requirements being reversed are not correlated. Because we use relative isolation, there is very little correlation between the two variables. Lastly, the method relies on there being very little signal in the Anti-Isolation and Anti-p_{T} regions. In our case, the MC predicts < 0.2 events in the Anti-p_{T} region (B), or $\sim 3\%$ of the predicted background in this control region.

The predicted number of QCD events in the Signal region can be calculated using the following equation:

$$n(A) = \frac{n(B) \times n(C) \times \mathrm{purity}(C)}{n(D)}. \quad (1)$$

The QCD-event purity in Equation 1 is calculated with respect to the other backgrounds expected in the control region (C). The purity is set to 1 as the other backgrounds are negligible.

The number of data events observed in each region is listed in Table 3. The method is also performed on the MC samples, shown here for reference but not used in the result. From the event numbers in the data, we estimate that the QCD background in region (A) is equal to 0.11 ± 0.11, completely compatible

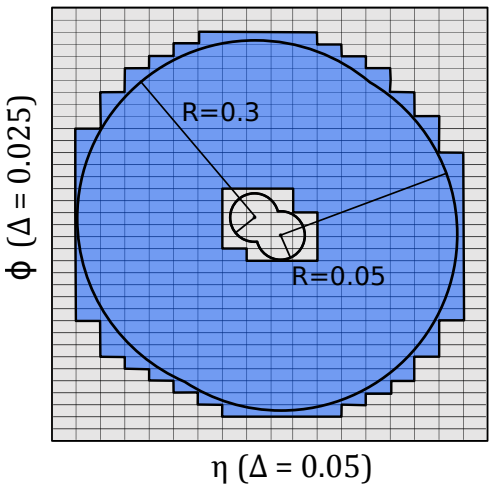

Figure 9: A cartoon illustrating the isolation calculation for lepton-jets. In this figure, the isolation is calculated in the 3^{rd} layer of the calorimeter for a lepton-jet containing two muons.

with the estimates from the probability-based QCD MC-sample estimate of 0.19 ± 0.19 from Section 4.2. No additional systematic was assigned to the background estimate as the two methods are in agreement.

Region	Number of Events in Data	Number of Events in QCD MC
(B) Anti-p_T	1	3.88 ± 3.88
(C) Anti-Isolation	3	1.46 ± 0.42
(D) Anti-Both	26	15.5 ± 2.9
(A) Signal Region	0	0.19 ± 0.19
	Prediction from method in Data	Prediction from method in MC
(A) Signal Region	0.11 ± 0.11	0.36 ± 0.36

Table 3: The number of data events observed in each of the four regions (A)-(D), together with the number of QCD data events predicted in the Signal region (A) by Equation 1. The right-hand column shows the corresponding numbers from the QCD MC sample, for which the simulated events were assigned the event weights described in Section 4.2.

5 Results and Systematics

5.1 Results

The number of data and simulated events in the analysis after each set of requirements are shown in Table 4. In the last three columns, the QCD background has been estimated using the QCD event weights in Section 4.2 to predict the effect of the high-quality muon requirements. For events with ≥ 4 muons, decaying from ≥ 2 dark-photons the acceptance varries between 8 and 30%, depending on the signal sample in question.

5.2 Systematic Uncertainties

The uncertainties in Table 4 are statistical only. To these, we add the following systematic uncertainties, expressed in Table 5.

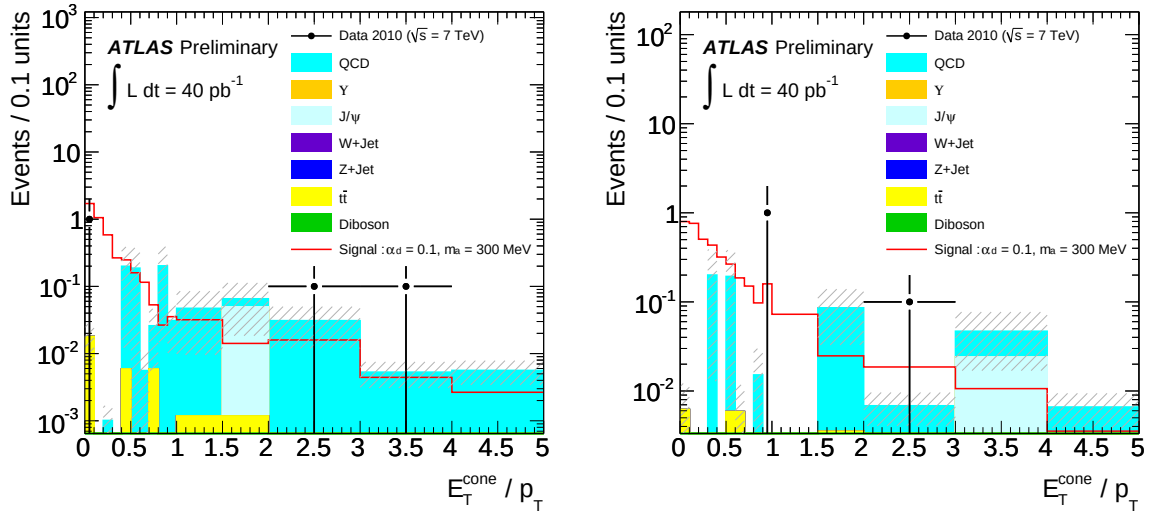

(a) (b)

Figure 10: (a) Distribution of the leading p_{T} lepton-jet scaled isolation after the trigger selection, requiring ≥ 4 muons, with ≥ 3 high-quality, and ≥ 2 lepton-jets. (b) The second-leading p_{T} lepton-jet distribution with the same requirements. The signal MC with dark-sector showering parameter $\alpha_d = 0.1$ and dark-photon mass $m_a = 300$ MeV is shown overlaid in red. Candidate events are required to have $E_T^{\mathrm{cone}}/p_T < 0.7$ in both of these plots. One event has second-leading lepton-jet scaled isolation > 5. The statistical error on the MC is represented by the grey hatched markings.

The integrated luminosity estimate of 40 pb^{-1} has a 3.4% systematic uncertainty associated with it. This systematic is applied to all samples, except for the QCD, J/Ψ, and Υ, as they are normalized using the data. In Section 3.2.1 we used the di-lepton events forming the Z mass peak to cross-check the impact of the luminosity uncertainty, as well as that of the trigger and reconstruction efficiency uncertainties. We found the level of disagreement between data and MC simulation in this cross-check to be about 3%.

The reconstruction efficiency for muons is measured via the tag-and-probe method using J/Ψ decays [26]. The muon reconstruction efficiency is fluctuated up and down by one sigma. From the change in acceptance, we compute a 2.9% systematic uncertainty on the number of events accepted. There is additionally a small systematic uncertainty on the trigger, which we conservatively round up to 1%.

The p_{T} measurements in the ID and MS of reconstructed muons in the MC simulation are smeared to match the resolution effects observed in data. The smearing function also returns a ± 1 sigma variation on each of the two values. The effect on the event yield for the MC samples varies from 0.9% to 0.1%, which we round up to 1%.

As discussed in Section 3.2.1, we assign a 4% systematic uncertainty per selected lepton-jet in the signal sample to cover the reconstruction efficiency as a function of ΔR.

The systematic uncertainties due to our imprecise knowledge of the theoretical cross-section on the contribution of the remaining backgrounds ($\sim 7\%$ for $t\bar{t}$ and $\sim 4\%$ for di-boson,) are small compared to their statistical errors, so although they are included, their impact is negligible.

6 Limits

Based on the results from the previous section, we compute 95% C.L. upper limits on the signal cross-section. They are calculated using the CL$_s$ method, implemented in COLLIE [27], using a log-likelihood-

	≥ 2 muon	≥ 4 muons	≥ 4 muons w/ ≥ 3 HQ	2 LJets	2 Isolated LJets
data	174450	246	84	3	0
all bkg	200000 ± 15000	200 ± 50	81 ± 20	1.74 ± 0.48	0.20 ± 0.19
QCD	160000 ± 14000	188 ± 50	73 ± 20	1.46 ± 0.42	0.19 ± 0.19
Υ	2100 ± 120	0.00 ± 0.00	0.00 ± 0.00	0.00 ± 0.00	0.00 ± 0.00
J/Ψ	22100 ± 3700	3.4 ± 1.9	0.95 ± 0.43	0.24 ± 0.23	0.00 ± 0.00
W+Jet	332 ± 11	0.40 ± 0.40	0.00 ± 0.00	0.00 ± 0.00	0.00 ± 0.00
Z+Jet	14420 ± 42	2.00 ± 0.50	1.37 ± 0.41	0.00 ± 0.00	0.00 ± 0.00
$t\bar{t}$	357 ± 1.4	4.31 ± 0.16	3.47 ± 0.14	0.041 ± 0.016	0.012 ± 0.008
Diboson	16.577 ± 0.070	1.640 ± 0.013	1.557 ± 0.013	0.00033 ± 0.00019	0.00033 ± 0.00019
Squark Signal Samples					
$\alpha_d = 0.0$, $m_a = 300$	8.26 ± 0.27	3.52 ± 0.18	2.38 ± 0.15	1.76 ± 0.12	1.38 ± 0.11
$\alpha_d = 0.0$, $m_a = 500$	6.90 ± 0.25	2.62 ± 0.15	1.87 ± 0.13	1.35 ± 0.11	1.04 ± 0.10
$\alpha_d = 0.1$, $m_a = 300$	15.16 ± 0.37	9.14 ± 0.28	7.58 ± 0.26	4.77 ± 0.21	2.90 ± 0.16
$\alpha_d = 0.1$, $m_a = 500$	15.97 ± 0.38	8.38 ± 0.27	6.99 ± 0.25	4.08 ± 0.19	2.33 ± 0.14
$\alpha_d = 0.3$, $m_a = 300$	9.60 ± 0.38	6.89 ± 0.32	5.99 ± 0.30	3.28 ± 0.22	1.25 ± 0.14
$\alpha_d = 0.3$, $m_a = 500$	11.75 ± 0.32	7.88 ± 0.26	7.01 ± 0.25	3.29 ± 0.17	1.11 ± 0.10

Table 4: The number of events in Data and MC at each stage of the analysis requirements. In the last three columns, the QCD background has been estimated using the QCD event weights to predict the effect of the high-quality muon requirements. HQ refers to high-quality muons in the table, α_d the dark-sector showering parameter, and m_a the dark photon mass. The reported errors are statistical only.

Systematic	Signal	QCD	J/Ψ	Υ	W+Jet	Z+Jet	$t\bar{t}$	Di-boson
Luminosity	3.4%				3.4%	3.4%	3.4%	3.4%
Trigger	1%				1%	1%	1%	1%
Reconstruction	2.9%				2.9%	2.9%	2.9%	2.9%
ΔR Efficiency	8%							
Muon Smearing	1%	1%	1%	1%	1%	1%	1%	1%
σ W					12%			
σ Z						1%		
σ $t\bar{t}$							7%	
σ Di-boson								4%

Table 5: The systematic uncertainties on the event yields for each sample. Note that we list here the systematics even for samples that are negligible after all requirements.

ratio test statistic, considering the statistical and systematic uncertainties of each sample. The results of the limit calculation are reported in Table 6. They are shown separately for the two mass points in Figure 11 for the cross-section times branching ratio to four muons, and in Figure 12 for the absolute cross-section.

7 Conclusion

We have presented a search for prompt, highly-collimated pairs of muons (lepton-jets), possibly along with softer, radiated leptons and/or mesons. The search was performed in 40 pb^{-1} of data, collected with the ATLAS detector in 2010.

The limits are calculated for specific parameters of our benchmark signal samples. We strove to keep the analysis as generic as possible, eschewing placing requirements on additional quantities such as the number of jets or $E_{\mathrm{T}}^{\mathrm{miss}}$, while at the same time keeping requirements such as those on the isolation of the lepton-jet as loose as possible.

Signal Point	Expected [pb]	68% Band [pb]	Observed [pb]
$\alpha_d = 0.00$, $m_a = 300$ MeV	0.31	0.43 - 0.26	0.26
$\alpha_d = 0.00$, $m_a = 500$ MeV	0.27	0.36 - 0.22	0.22
$\alpha_d = 0.01$, $m_a = 300$ MeV	0.36	0.49 - 0.31	0.31
$\alpha_d = 0.01$, $m_a = 500$ MeV	0.37	0.48 - 0.31	0.31
$\alpha_d = 0.03$, $m_a = 300$ MeV	1.5	2.1 - 1.3	1.3
$\alpha_d = 0.03$, $m_a = 500$ MeV	1.5	2.0 - 1.2	1.2

Table 6: The expected and observed 95% C.L. upper limits on the production cross-section times branching ratio to four muons for the simulated signal samples. Also reported are the bands containing 68% of background-only psuedo-experiments. The limits are expressed for the simulated dark-sector showering parameter and dark photon mass signal points.

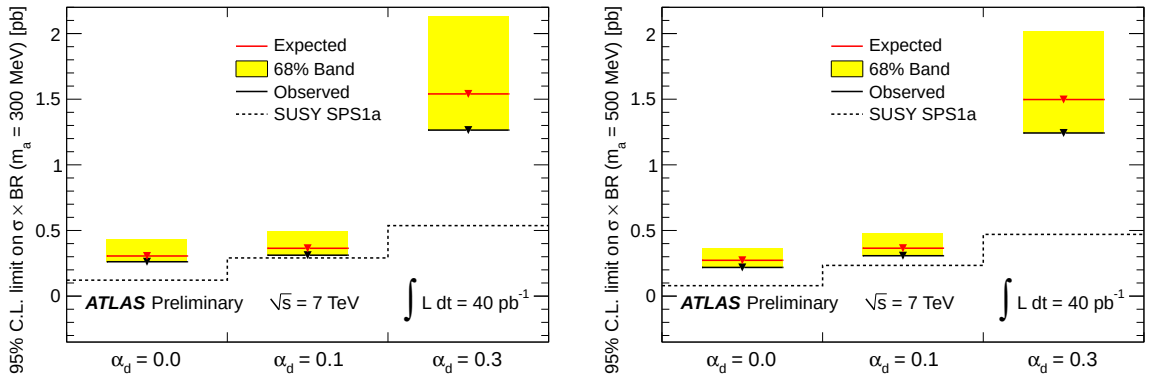

(a) (b)

Figure 11: The expected and observed 95% C.L. limits on the production cross-section times branching ratio to four muons for the simulated signal samples with dark photon mass (a) $m_a = 300$ MeV, and (b) $m_a = 500$ MeV. The y-axis is the limit on the cross-section times branching ratio. The x-axis is the dark-sector showering parameter. The yellow bands contain 68% of background-only psuedo-experiments.

Zero signal candidates were found after all selection criteria were applied to the data. This observation is consistent with the SM background prediction of 0.20 +- 0.19 events, which is dominated by QCD multi-jet production. Consequently we set 95% C.L. limits on the cross-section times branching ratio of new physics that produces this final state. The analysis was performed using data-driven estimates of efficiencies and backgrounds when possible.

For decays of hidden-valley dark photons originating from pair-production of squarks, assuming the SPS1a benchmark for the SUSY parameters [20], the most stringent limits are set in the case where α_d (the dark-sector showering parameter) is 0.0 and m_a (the dark photon mass) is 500 MeV. In this scenario, the observed (expected) 95% C.L. upper limit is 0.22 pb (0.27 pb), or 2.6 (3.2) times the theoretical cross-section times branching fraction. In the least sensitive case, where $\alpha_d = 0.3$ and $m_a = 300$ MeV, the observed (expected) upper limit is 1.3 pb (1.5 pb), or 2.4 (2.7) times the theoretical cross-section times branching ratio to four muons. Our results are similar to the recent preliminary results from CMS [13], which range from $\sim$0.1 to 0.5 pb. The D0 limits [12], when extrapolated to LHC energies are of order 1 pb.

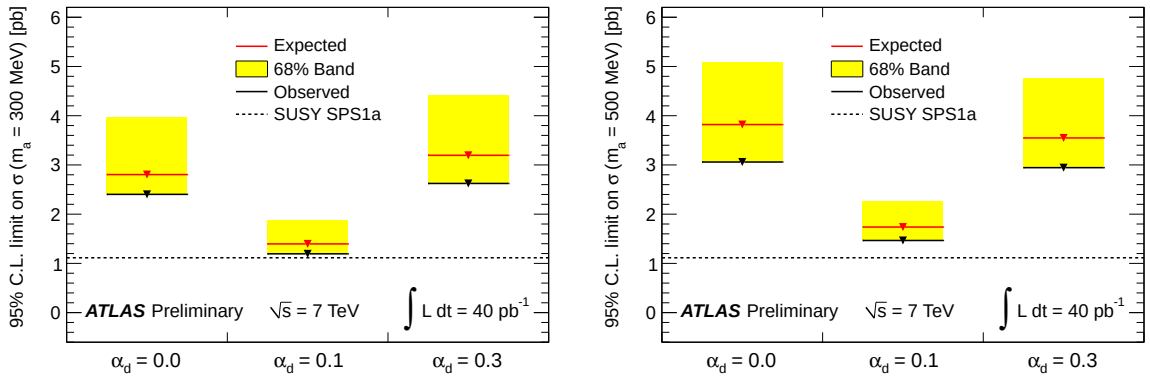

(a) (b)

Figure 12: The expected and observed 95% C.L. limits on the production cross-section for the simulated signal samples with dark photon mass (a) $m_a = 300$ MeV with BR($\gamma_d \to \mu\mu$) = 0.47, and (b) $m_a = 500$ MeV with BR($\gamma_d \to \mu\mu$) = 0.4. The y-axis is the limit on the cross-section. The x-axis is the dark-sector showering parameter. The yellow bands contain 68% of background-only psuedo-experiments.

References

[1] A. A. Abdo et al., *Measurement of the Cosmic Ray e^+e^- Spectrum from 20 GeV to 1 TeV with the Fermi Large Area Telescope*, Phys. Rev. Lett. **102** (2009) 181101.

[2] O. Adriani et al., *An anomalous positron abundance in cosmic rays with energies 1.5 - 100 GeV*, Nature **458** (2009) 607, arXiv:0810.4995 [astro-ph].

[3] J. Chang et al., *An excess of cosmic ray electrons at energies of 300 - 800 GeV*, Nature **456** (2008) 362. http://dx.doi.org/10.1038/nature07477.

[4] R. Bernabei, P. Belli, F. Cappella, R. Cerulli, C. J. Dai, A. d'Angelo, H. L. He, A. Incicchitti, H. H. Kuang, X. H. Ma, F. Montecchia, F. Nozzoli, D. Prosperi, X. D. Sheng, R. G. Wang, and Z. P. Ye, *New results from DAMA/LIBRA*, Eur. Phys. J. C **67** (Feb, 2010) 39–49, arXiv:1002.1028 [astro-ph.GA].

[5] The CDMS II Collaboration, *Dark Matter Search Results from the CDMS II Experiment*, Science **327** (March, 2010) 1619–1621. http://dx.doi.org/10.1126/science.1186112.

[6] N. Arkani-Hamed, D. P. Finkbeiner, T. R. Slatyer, and N. Weiner, *A Theory of Dark Matter*, Phys. Rev. D **79** (2009) 015014, arXiv:0810.0713 [hep-ph].

[7] M. Baumgart, C. Cheung, J. T. Ruderman, L.-T. Wang, and I. Yavin, *Non-Abelian Dark Sectors and Their Collider Signatures*, JHEP **04** (2009) 014, arXiv:0901.0283 [hep-ph].

[8] D. S. M. Alves, S. R. Behbahani, P. Schuster, and J. G. Wacker, *Composite Inelastic Dark Matter*, arXiv:0903.3945 [hep-ph].

[9] G. D. Kribs, T. S. Roy, J. Terning, and K. M. Zurek, *Quirky Composite Dark Matter*, Phys. Rev. D **81** (Sep, 2010) 095001, arXiv:0909.2034 [hep-ph].

[10] A. Katz and R. Sundrum, *Breaking the dark force*, Journal of High Energy Physics **2009** (June, 2009) 003+, arXiv:0902.3271 [hep-ph].

[11] A. Falkowski, J. T. Ruderman, T. Volansky, and J. Zupan, *Hidden Higgs Decaying to Lepton Jets*, arXiv:1002.2952 [hep-ph].

[12] DØ Collaboration, V. M. Abazov et al., *Search for events with leptonic jets and missing transverse energy in $p\bar{p}$ collisions at $\sqrt{s} = 1.96$ TeV*, Phys. Rev. Lett. **105** (2010) 211802, arXiv:1008.3356 [hep-ex].

[13] CMS Collaboration, *Search for Resonant Production of Lepton Jets*, https://twiki.cern.ch/twiki/bin/view/CMSPublic/PhysicsResultsEXO11013, March, 2011.

[14] ATLAS Collaboration, *The ATLAS Experiment at the CERN Large Hadron Collider*, Journal of Instrumentation **3** (2008) S08003. http://dx.doi.org/10.1088/1748-0221/3/08/S08003.

[15] ATLAS Collaboration, *Updated Luminosity Determination in pp Collisions at $\sqrt{s} = 7$ TeV using the ATLAS Detector*, ATLAS-CONF-2011-011 (2011) .

[16] I. Yavin, *Lepton Jet Studies*, http://astro.physics.nyu.edu/~iyavin/LeptonJets/, September, 2009.

[17] C. Cheung, J. T. Ruderman, L.-T. Wang, and I. Yavin, *Lepton Jets in (Supersymmetric) Electroweak Processes*, JHEP **04** (2010) 116, arXiv:0909.0290 [hep-ph].

[18] J. Alwall, P. Artoisenet, S. de Visscher, C. Duhr, R. Frederix, M. Herquet, and O. Mattelaer, *New Developments in MadGraph/MadEvent*, arXiv:0809.2410 [hep-ph].

[19] T. Sjostrand, S. Mrenna, and P. Z. Skands, *PYTHIA 6.4 Physics and Manual*, JHEP **0605** (2006) 026, arXiv:hep-ph/0603175 [hep-ph].

[20] B. Allanach, G. Blair, A. Freitas, S. Kraml, H. Martyn, G. Polesello, W. Porod, and P. Zerwas, *SUSY Parameter Analysis at TeV and Planck Scales*, Nuclear Physics B - Proceedings Supplements **135** (Oct., 2004) 107–113. http://dx.doi.org/10.1016/j.nuclphysbps.2004.09.052.

[21] S. Frixione and B. R. Webber, *Matching NLO QCD computations and parton shower simulations*, Journal of High Energy Physics **2002** (June, 2002) 029+, arXiv:hep-ph/0204244 [hep-ph].

[22] S. Agostinelli, *Geant4 a simulation toolkit*, Nuclear Instruments and Methods in Physics Research Section A: Accelerators, Spectrometers, Detectors and Associated Equipment **506** (July, 2003) 250–303. http://dx.doi.org/10.1016/S0168-9002(03)01368-8.

[23] J. Allison et al., *Geant4 developments and applications*, IEEE Transactions on Nuclear Science **53** (February, 2006) 270–278. http://dx.doi.org/10.1109/TNS.2006.869826.

[24] ATLAS Collaboration, *Single Boson and Diboson Production Cross Sections in pp Collisions at $\sqrt{s} = 7$ TeV*, ATL-COM-PHYS-2010-695 (2010) .

[25] B. Lenzi, R. Nicolaidou, and S. Hassani, *TrackInCaloTools: A package for measuring muon energy loss and calorimetric isolation in ATLAS*, Journal of Physics: Conference Series **219** (2010) 032049. http://dx.doi.org/10.1088/1742-6596/219/3/032049.

[26] ATLAS Collaboration, *Muon Momentum Resolution in First Pass Reconstruction of pp Collision Data Recorded by ATLAS in 2010*, ATLAS-CONF-2011-046 (2011) .

[27] W. Fisher, *Collie: A Confidence Level Limit Evaluator*, D0 note 5595.